Journal of Power Sources 264 (2014) 211–219

Contents lists available at ScienceDirect

Journal of Power Sources

journal homepage: www.elsevier.com/locate/jpowsour

Reliability assessment for components of large scale photovoltaic systems

Amir Ahadi [a,*], Noradin Ghadimi [a], Davar Mirabbasi [b]

[a] Young Researchers Club, Ardabil Branch, Islamic Azad University, Ardabil, Iran
[b] Department of Electrical Engineering, Ardabil Branch, Islamic Azad University, Ardabil, Iran

HIGHLIGHTS

- This paper presents a complete and real structure of the large-scale PV systems.
- FTA is used to analyze the effects of a battery system on the system reliability.
- We estimate total component reliability and overall reliability for the PV system.
- Increasing nominal power output of the PV system will decrease Reliability.
- The critical components with priority for the PV system are revealed.

ARTICLE INFO

Article history:
Received 23 September 2013
Received in revised form
15 March 2014
Accepted 11 April 2014
Available online 26 April 2014

Keywords:
Reliability assessment
Photovoltaic
Fault tree method
Analytical models

ABSTRACT

Photovoltaic (PV) systems have significantly shifted from independent power generation systems to a large-scale grid-connected generation systems in recent years. The power output of PV systems is affected by the reliability of various components in the system. This study proposes an analytical approach to evaluate the reliability of large-scale, grid-connected PV systems.

The fault tree method with an exponential probability distribution function is used to analyze the components of large-scale PV systems. The system is considered in the various sequential and parallel fault combinations in order to find all realistic ways in which the top or undesired events can occur. Additionally, it can identify areas that the planned maintenance should focus on. By monitoring the critical components of a PV system, it is possible not only to improve the reliability of the system, but also to optimize the maintenance costs. The latter is achieved by informing the operators about the system component's status. This approach can be used to ensure secure operation of the system by its flexibility in monitoring system applications. The implementation demonstrates that the proposed method is effective and efficient and can conveniently incorporate more system maintenance plans and diagnostic strategies.

1. Introduction

Analyzing the reliability of PV power systems is important for planning and long-term operation, because the analysis helps predict system behavior over time and devise appropriately timed maintenance plans. It is a significant factor for the operator to be able to assess system reliability under long-term operations in order to optimize decisions in design, engineering, procurement, construction, and service [1].

PV and wind systems produce electric power, which involves zero greenhouse gas emissions and fossil fuel consumption. The total capacity of grid-connected PV power systems has grown exponentially, from 300 MW in 2000 to approximately 67 GW in 2011 [2]. PV power generation will become the main focus of future energy development. As a clean energy, its application has gradually changed toward large-scale, grid-connected systems. It significantly influences the reliability, economics and operational stability of such systems [3]. The largest PV system with a generation capacity of 80 MW was installed in Sarnia, Ontario, Canada, in 2010 [4]. Additionally, the European PV Technology Platform Group

* Corresponding author.
E-mail addresses: amirahadi8@gmail.com (A. Ahadi), noradin.ghadimi@gmail.com (N. Ghadimi), dmirabbasi@yahoo.com (D. Mirabbasi).

http://dx.doi.org/10.1016/j.jpowsour.2014.04.041
0378-7753/

Nomenclature

I_{ph}	internal equivalent current source
V_t	thermal voltage of the array
q	the electron charge of 1.602×10^{-19} Coulomb
T_j	the temperature of the pn junction
G	solar irradiation
ΔT	temperature deviation from the reference value
T_n	reference temperature
I_{sr}	the reference reverse saturation current
MPP	maximum power point
I_{SC}	PV short-circuit current
$V_{mpp,max}$	maximum MPP voltage of the inverter
μ_I	PV temperature coefficient of I_{SC}
I_{mpp}	PV current at the maximum power point
$I_{DC,max}$	maximum input DC current of the inverter
$F(t)$	failure probability function
ACS, DCS	AC or DC switch
CB	AC circuit breaker
INV	inverter
CON	connector
CC	charge controller
FV	Fussel–Vesely
$Pr(E)$	failure probability
P_{TOP}	the probability of top event
P_{MCS_i}	the probability of occurrence of MCS_i
$P_{B1}, P_{B2},\ldots P_{Bn}$	the failure probabilities of basic events
M	number of batteries in parallel
T	the system's time to failure
$\lambda_{Battery}$	failure rate of the battery system
I_s	reverse saturation current
N_s	cells connected in series
k	the Boltzmann constant of 1.38×10^{-23} J K^{-1}
a	the permittivity of the diode
K_i	temperature coefficient (mA °C^{-1})
G_n	the reference irradiation
E_g	bandgap energy of the semiconductor
P_{max}	maximum output power of a PV cell
$V_{mpp,min}$	minimum MPP voltage of the inverter
V_{mpp}	PV voltage at the maximum power point
V_{oc}	PV open-circuit voltage
μ_V	PV temperature coefficient of V_{oc}
V_{max}	maximum operating voltage of the inverter
$R(t)$	reliability probability function
$f(t)$	probability density function
GP	grid protection
SPD	surge protection device
BD	blocking diode
PV	photovoltaic cell
BS	battery system
DCB	differential circuit breaker
$1 - Pr(E)$	reliability probability
MCS_i	minimal cut set i
m	the number of basic events in the largest minimal cut set
n	the number of minimal cut sets
N	total number of batteries
E_i	the event that component i operates without failure
$\lambda_{Charge-Controller}$	failure rate of the charge controller

reports that PV systems are predicted to reach network parity in most of Europe in 2019 [5].

In recent literature, evaluating the reliability of solar PV has been a point of interest.

In Ref. [6], the investigators analyzed the reliability of solar PV power system designs using failure mode effect analysis (FMEA) and fault tree analysis (FTA), and also calculated the failure rates of the PV array and inverter. In Ref. [7], the investigators estimated reliability equations from the FTA but did not analyze the reliability probability functions. The maximum reliability of PV arrays with optimal interconnection of PV modules was investigated in Ref. [8–10]. In Ref. [11], the researchers evaluated the reliability of an electric power generation system, including a PV system, by considering the load under the assumption that none of the system components ever failed. The researchers in Ref. [12] proposed a new method for the calculation of the optimal configuration of large-scale PV systems. In Ref. [13], FTA and Markov chain method are jointly used to evaluate the behavior of PV system. The energy cost of PV system is estimated and applied to PV system designs. The investigators in Ref. [14] studied the reliability of battery voltage regulators (BVRs) used in PV systems and calculated the overall system reliability. In Ref. [15], the investigators proposed a model using Monte Carlo for the analysis of reliability of rechargeable batteries in photovoltaic power supply systems. In Ref. [16], the researchers discussed the PV inverters used in PV systems, presenting their experimental results. The reliability of PV systems was estimated in various small-scale field tests described in Refs. [17–19].

Although a wide variety of studies have been conducted about the large-scale, grid-connected PV systems [20–27], the real electrical architecture of modern large-scale, grid-connected PV systems with battery backup requires further consideration.

This paper presents a technique for analyzing the reliability of large-scale, grid-connected PV systems using an exponential distribution based on FTA method and considering the presence of a battery system and charge controller. It is necessary to point out that changing the function from exponential distribution to, for example, accelerated life tests (ALTs) with Log-normal, Weibull or mixed-Weibull distributions did not alter the output of the proposed method. In addition, if the repair interval of the system components is sufficiently less than a critical value and does not influence the system operation, then the repair time could be ignored. Thus, in this study, it was assumed that any failures could not be repaired [7], [11], and [28–32]; therefore, if a component failed, the overall PV system was assumed to be in failure mode and the repair is finished during a short time. However, the overall system remaining in operation during that time, because the electric power of distribution system is sufficient for loads to use. It is also important to point out that in order to define the critical components, the scope of this paper is focused on the reliability evaluation of PV systems based on unrepairable components. It is assumed the repair time of the system failure is too short and the loads could be incorporated with the distribution system during failure. However, the proposed method is applicable when the repair and the common-cause degradation are considered.

The remainder of the paper is organized as follows. Section 2 describes the electrical structure of large-scale grid connected PV systems. Section 3 proposes the reliability modeling formulation. The case studies are presented in Section 4. Finally, the conclusions are provided in Section 5.

2. Large-scale photovoltaic systems

The electrical structure of a large scale PV system is shown in Fig. 1. The PV power generation model should be drastically derived as a function of solar irradiation and surface temperature of solar panels in order to determine the solar power generation more efficiently [24]. The equivalent circuit of the PV module is shown in Fig. 2.

The I–V characteristic of a PV cell is expressed as:

$$I_{PV} = I_{ph} - I_s\left[\exp\left(\frac{V_{PV} + R_s \times I_{PV}}{V_t \times a}\right) - 1\right] - \frac{V_{PV} + R_s \times I_{PV}}{R_{sh}} \quad (1)$$

where

$$V_t = \frac{N_s \times k \times T_j}{q}. \quad (2)$$

Both the PV output current and saturation current change with the solar radiation and panel temperature. Thus, the PV internal equivalent current source can be expressed as:

$$I_{ph} = (I_{SC} + K_i \times \Delta T) \times \frac{G}{G_n} \quad (3)$$

The reverse saturation current can be also represented as follows:

$$I_s = I_{sr}\left(\frac{T_n}{T_j}\right)^3 \exp\left[\frac{q \times E_g}{a \times k}\left(\frac{1}{T_n} - \frac{1}{T_j}\right)\right] \quad (4)$$

The maximum output power of a PV cell is then expressed by

$$\begin{aligned} P_{max} &= V_{PV} \times I_{PV} \\ &= V_{PV} \times \left(I_{ph} - I_s\left[\exp\left(\frac{V_{PV} + R_s \times I_{PV}}{V_t \times a}\right) - 1\right] \right.\\ &\left. - \frac{V_{PV} + R_s \times I_{PV}}{R_{sh}}\right). \end{aligned} \quad (5)$$

The modeling of a solar module is discussed in more details in Ref. [33]. Seven large-scale PV systems, with nominal power output from 100 kW to 2500 kW, are used in order to calculate the overall system reliability. The PV module and inverter characteristics which listed in Table 1, are the same in all systems.

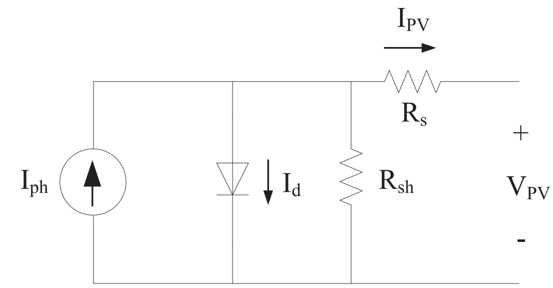

Fig. 2. Equivalent circuit of the photovoltaic cell.

Table 1
The PV module and inverter characteristics.

Inverter (100 kW)	PV module (230 W)
$V_{mpp,min} = 450$ V	$I_{SC} = 8.24$ A
$V_{mpp,max} = 820$ V	$V_{mpp} = 30.2$ V
$V_{max} = 1000$ V	$\mu_I = 3.3$ mA °C^{-1}
$I_{DC,max} = 235$ A	$V_{oc} = 37.2$ V
	$I_{mpp} = 7.60$ A
	$\mu_v = -120$ mV °C^{-1}

To ensure that no inverse current is running in a string, the PV module strings are connected to the inverter by means of a protection. The protection can be a blocking diode (as shown in Fig. 1), a fuse or a circuit breaker. After the string protection, the DC switch helps to disconnect the PV field for maintenance, even under solar irradiation. After the DC switch, the charge controller regulates the power coming from the solar panels to the batteries and prevents the batteries from over-charging. Then, the battery system stores the generated energy for emergency use at night and on cloudy days. To convert from DC to AC, inverters are added, which are protected from lightning by surge protection devices (SPDs). To protect the AC lines, as per normal electrical design practice, an AC circuit breaker is added after the inverter. Ultimately, the PV system is connected to the transformer, though that was not done in this study. Table 2 reports the number of components in each PV system, which increased as the system's nominal power output increased. Note that in real-world installations, some devices could be eliminated. In order to focus only on failures of electrical and electronics components, the failure of cables was not considered. Therefore, the analysis assumed a flawless system installation, as

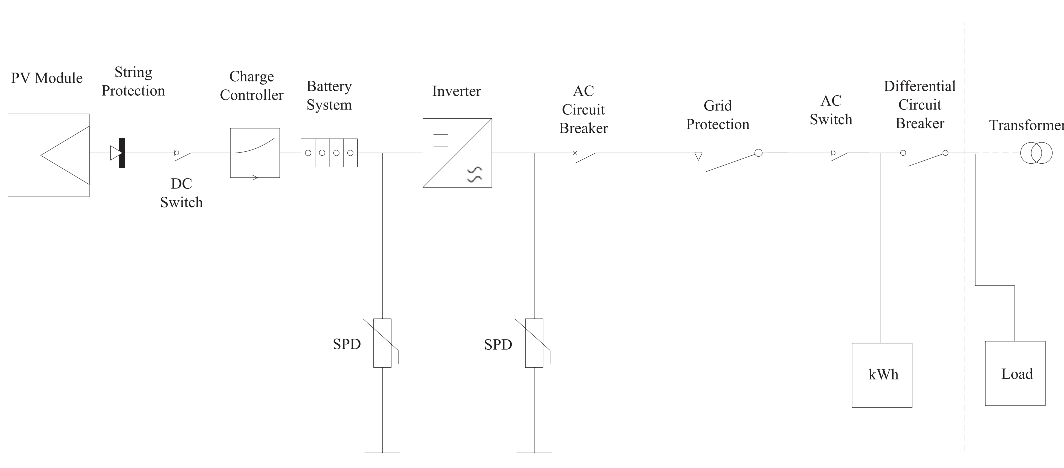

Fig. 1. Electrical structure of the large scale PV system.

Table 2
Number of components per each PV system.

Power (kW)	100	200	500	1000	1500	2000	2500
PV modules	437	874	2166	4351	6517	8702	10,868
String protection	23	46	114	229	343	458	572
DC switch	3	6	15	27	42	57	72
Inverter	1	2	5	9	14	19	24
AC circuit breaker	1	2	5	9	14	19	24
Grid protection	1	1	1	1	1	1	1
AC switch	1	1	1	1	1	1	1
Differential circuit breaker	1	1	1	1	1	1	1
Connector (couple)	874	1748	4332	8702	13,034	17,404	21,736
Battery system	16	30	76	150	224	298	372
Charge controller	1	1	1	1	1	1	1

well as flawless SPDs with no failure rates. The reliability of all seven PV systems was analyzed over one year of operation and over 20 years operation with 8.5 h of operation per day. Therefore, the failure rates for all components are failures hour^{-1}.

The batteries used in this study came from the Rolls–Surrette factory. All PV systems used an identical battery model, Ah and voltage, 12 CS 11P, 475 Ah and 12 V, respectively. Many installation methods can calculate the number and structure of batteries in PV systems [34]; however, in this study, it was assumed that each battery system had two days of reserve capacity. It is also important to point out that considering the overall PV power output as a reserve capacity is not economical. Therefore, the analysis considered only the emergency reserve needed in PV systems, which was assumed to be 5% of the PV power output for all PV systems. The battery system consisted of two batteries in series, each with a nominal voltage of 12, for a total required voltage of 24 and M batteries in parallel.

For instance, the method used to determine the number of batteries in the battery bank for a 200 kW PV system is described as follows:

1. Determining the emergency reserve needed ($5\% \times 200 \times 10^3$ W = 10,000 W).
2. Defining the number of reserved days (2 days).
3. The third step is to determine the watt hours needed during periods of little or no sunshine (10,000 W × 2 days × 8.5 h = 170,000 W h).
4. Determining the amp hours needed in the periods of no sunshine from dividing the watt hour in step three by the battery system voltage (170,000 W h/12 V = 14 250 Ah).
5. Dividing the amp hour calculated in the step four by the battery system amp hour in order to determine the total number of batteries (14,250 Ah/475 Ah = 30). Then, divide this by 2 in order to determine the total number of batteries in parallel (30/2 = 15).

This steps can be summarized as follows:

$$N = \frac{(200\ \mathrm{kW} \times 2\ \mathrm{days} \times 8.5\ \mathrm{h} \times 5\%)/12\ \mathrm{V}}{475\ \mathrm{Ah}} = 30 \tag{6}$$

$$M = 30/2 = 15 \tag{7}$$

3. Basic reliability concepts and mathematics

3.1. General reliability function

Reliability is defined in quantitative terms as the probability of a component performing its function adequately. The reliability function is the probability that a system will be successfully operating without any failure in the given time t:

$$R(t) = P(T > t) \tag{8}$$

The unreliability or failure probability can be also expressed as:

$$F(t) = P(T \le t) = 1 - R(t) \tag{9}$$

Equations (8) and (9) with a density function $f(t)$ could be written as:

$$R(t) = \int_t^{\infty} f(t)\mathrm{d}t \tag{10}$$

$$F(t) = \int_{-\infty}^{t} f(t)\mathrm{d}t \tag{11}$$

The mean time to failure (MTTF) of a component can be expressed as:

$$\mathrm{MTTF} = \int_0^{\infty} t \times f(t)\mathrm{d}t = \int_0^{\infty} R(t)\mathrm{d}t \tag{12}$$

Equation (12) represents the reliability of a component. In the real world, systems are complex and consist of a large number of components that may be connected in series, in parallel or in a combination of series and parallel. When connected in series, the failure of one component interrupts the overall system, whereas all components must fail in the parallel system to interrupt the overall system.

The reliability of a series system with n components can be calculated as:

$$R_{\mathrm{system}} = P[E_1 \cap E_2 \cap \cdots \cap E_i] \tag{13}$$

If the n components are independent, thus:

$$R_{\mathrm{system}} = P(E_1) \times P(E_2) \cdots \times P(E_i) \tag{14}$$

Assuming the system is not repairable [32], the overall system reliability can always be derived by Boolean techniques. Thus, system reliability performance can be expressed as a function of components reliability as follows:

$$R_{\mathrm{system}} = R_1 \times R_2 \times \ldots R_n \tag{15}$$

Thus

$$R_{\mathrm{system}} = \prod_{i=1}^{n} R_i \tag{16}$$

where $R_i = P(E_i)$ is the reliability of component i.

The system reliability of x series units with M parallel components in each unit can be obtained using:

$$R_{\mathrm{system}} = 1 - (1 - R^x)^M \tag{17}$$

A detailed discussion of the existing technique can be found in Refs. [38–40].

The reliability data were taken from Refs. [18] and [21–37]. The failure rates of the battery system and the charge controller were 0.08 and 0.04 for 2 years, respectively [36]; hence, the failure rates were calculated as:

$$\lambda_{Battery} = 0.08/2/365/8.5 = 12.89 \times 10^{-6} \text{ failures h}^{-1} \quad (18)$$

$$\lambda_{Charge-controller} = 0.04/2/365/8.5 = 6.44 \times 10^{-6} \text{ failures h}^{-1} \quad (19)$$

All failure rates appear in Table 3.

3.2. Fault tree method

The fault tree method (FTA) is the most useful tool in analyzing the risk and reliability of causal systems. FTA is a graphical design method in which failures are defined more easily than non-failures. The focus is usually on a failure appearing at the top of the fault tree diagram. One of the major advantages of FTA is that it can predict the most system failures in a system breakdown. FTA attempts to associate failure processes of logic diagrams, which show the state and behavior of the system. The top event defines the failure mode of the system or its function, which is then analyzed in terms of failure modes of its components and influence factors [41]. The top event of a fault tree should be considered carefully. If it is selected, the analysis generally becomes unmanageable, and its success is not guaranteed. To clarify the advantages of proposed approach, a simplified fault tree of a distribution system with a probability of P_A, a protection system with a probability of P_B, restoring upstream customers with a probability of P_C, and restoring downstream customers with a probability of P_D, is given in Fig. 3. Each combination of successful and unsuccessful system responses corresponds to a path on the FTA, and the probability of any outcomes are calculated by multiplying the associated probabilities of each individual system response [42].

A fault tree also is assigned by "gates" that present the relationships between their input and output events. A detailed discussion of fault tree techniques is outside the scope of this study but can be found in Ref. [43].

Fig. 4 shows a fault tree for the PV system illustrated in Fig. 1.

A system may have more than one top event, as shown in Fig. 4. The top event appears in a box that represents the failure event under investigation. For instance, Energy reduced if PV irradiated was determined as a top event in this study.

The following basic symbols are used in Fig. 4 to represent the relationship between the top event and lower level events:

- OR gate: The event above the gate will occur if at least one combination of the input events (the events shown below the gate) exist.
- Rectangle: The rectangle, the main block of FTA, represents a negative event. It is located at the top of the tree or throughout the tree to denote other events of interest.

Table 3
Component failure rates.

Component	Failure rate (10^{-6} failures h^{-1})	Reference
PV modules	0.0152	[18]
String protection	0.313	[35] Sect. 6-2
DC switch	0.2	[35] Sect. 22-1
Inverter	40.29	[21]
AC circuit breaker	5.712	[35] Sect. 14-5
Grid protection	5.712	[35] Sect. 14-5
AC switch	0.034	[35] Sect. 14-1
Differential circuit breaker	5.712	[35] Sect. 14-5
Connector (couple)	0.00024	[35] Sect. 17-1
Battery system	12.89	[36]
Charge controller	6.44	[36]

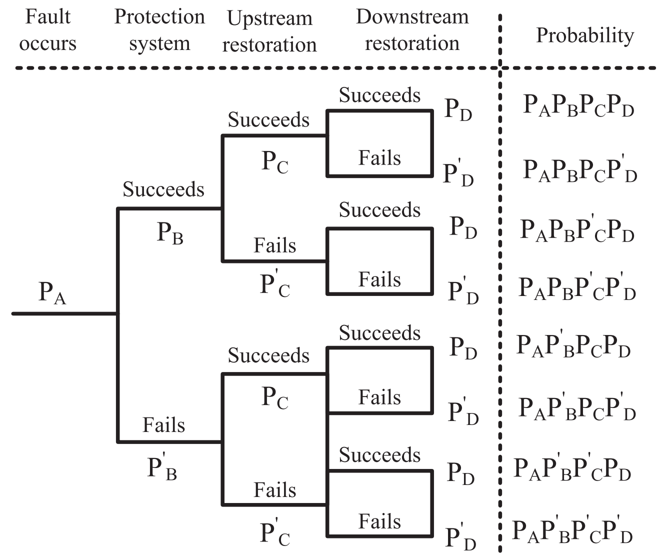

Fig. 3. A simplified fault tree.

- Circle: A circle is a base event in the tree and does not require any gates or events as inputs.

3.3. Minimal cut sets evaluation using FTA

In this section, a mathematical model for cut sets is presented using FTA. Such methods significantly help to convert fault trees into Boolean models and mathematical equations. By definition, a minimal cut set causes the system to be unavailable because of component failures. If all components are unavailable, a minimal cut set will cause the top event to occur. If all components are available, then the top event will not occur. The minimal cut set for any fault tree is finite and can be achieved easily. For instance, the three component minimal cut sets show that all three components must fail in order for the top event to occur. For an n component minimal cut set, all n components must be unavailable [43].

The minimal cut set expression for the top event can be obtained from Fig. 4 as:

$$\begin{aligned}\text{Top event} = {} & ((((((((\text{PV} + \text{CON} + \text{BD}) + \text{DCS}) + \text{CC}) \\ & + (\text{SPD} + \text{BS})) + \text{INV}) + (\text{CBac} + \text{SPD})) + \text{GP}) \\ & + \text{ACS}) + \text{DCB})\end{aligned} \quad (20)$$

It is also assumed that SPDs are flawless and have no failure rates; therefore, Equation (20) is reduced to:

$$\begin{aligned}\text{Top event} = {} & \text{PV} + \text{CON} + \text{BD} + \text{DCS} + \text{CC} + \text{BS} + \text{INV} + \text{CBac} \\ & + \text{GP} + \text{ACS} + \text{DCB}\end{aligned} \quad (21)$$

Equation (21) indicates that the fault tree in this study had 11 minimal cut sets. The analysis of the FTA can be categorized into the two kinds of qualitative and quantitative analysis. The qualitative analysis is obtained from minimal cut sets (the combinations of events which can cause system failure) and quantitative fault tree evaluation deals with calculating the top event probability according to the bottom events [44]. The probability of failure for top event can be calculated on qualitative analysis as follows [41]:

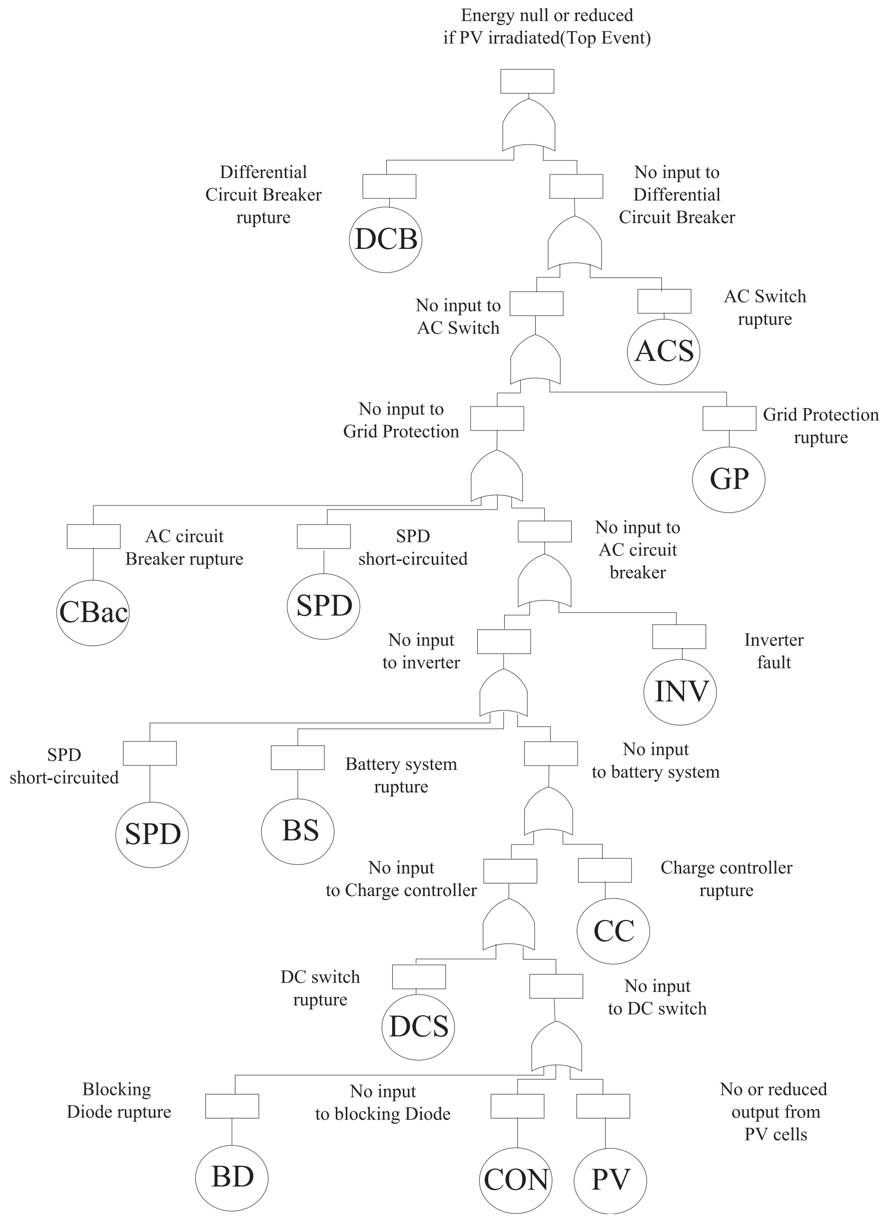

Fig. 4. Fault tree for the PV system in Fig. 1.

$$P_{\mathrm{TOP}} = \sum_{i=1}^{n} P_{\mathrm{MCS}_i} - \sum_{i<j} P_{\mathrm{MCS}_i \cap \mathrm{MCS}_j} + \sum_{i<j<k} P_{\mathrm{MCS}_i \cap \mathrm{MCS}_j \cap \mathrm{MCS}_k} - \cdots + (-1)^{m-1} P \bigcap_{i=1}^{m} \mathrm{MCS}_i \quad (22)$$

The probability of occurrence of MCS_i can be expressed as:

$$P_{\mathrm{MCS}_i} = P_{B1} \times P_{B2} | P_{B1} \times P_{B3} | P_{B1} \cap P_{B2} \times \cdots \times P_{Bn} | P_{B1} \cap P_{B2} \cap \cdots \cap P_{Bn-1} \quad (23)$$

It was assumed that the components are independent. Thus,

$$P_{\mathrm{MCS}_i} = \prod_{i=1}^{n} P_{Bi} \quad (24)$$

Using probability theory and the minimal cut set, the probability of failure of the top event can be obtained from Equation (21), and the reliability probability can be expressed as:

$$Pr(\text{Top event}) = Pr(E_1 + E_2 \ldots E_n) \quad (25)$$

$$1 - Pr(\text{Top event}) = [1 - Pr(E_1)] \times [1 - Pr(1 - E_2)] \ldots [1 - Pr(1 - E_n)] \quad (26)$$

It is assumed that the components are independent, so the total system reliability can be calculated as:

$$R_{\mathrm{tot}} = \prod_{i=1}^{n} = R(\mathrm{PV}) \times R(\mathrm{CON}) \times R(\mathrm{BD}) \times R(\mathrm{DCS}) \times R(\mathrm{CC}) \times R(\mathrm{BS}) \times R(\mathrm{INV}) \times R(\mathrm{CBac}) \times R(\mathrm{GP}) \times R(\mathrm{ACS}) \times R(\mathrm{DCB}) \quad (27)$$

Using exponential distribution and Equation (16), the total system reliability can be shown as:

Table 4
Total component reliability for the PV systems for a period of one year of operations [in %].

Power (kW)	100	200	500	1000	1500	2000	2500
PV modules	97.9603	95.9622	90.2899	81.4497	73.5409	66.3405	59.8988
String protection	97.7913	95.6313	89.5204	80.0613	71.6712	64.0981	57.3809
DC switch	99.8140	99.6284	99.0736	98.3386	97.4276	96.5250	95.6307
Inverter	88.2497	77.8801	53.5262	32.4653	17.3775	9.3015	4.9787
AC circuit breaker	98.2435	96.5178	91.5205	85.2576	78.0281	71.4117	65.3564
Grid protection	98.2435	98.2435	98.2435	98.2435	98.2435	98.2435	98.2435
AC switch	99.9895	99.9895	99.9895	99.9895	99.9895	99.9895	99.9895
Differential circuit breaker	98.2435	98.2435	98.2435	98.2435	98.2435	98.2435	98.2435
Connector (couple)	99.9349	99.8699	99.6780	99.3541	99.0342	98.7125	98.3946
Battery system	99.9996	99.9992	99.9981	99.9962	99.9942	99.9923	99.9904
Charge controller	98.0218	98.0218	98.0218	98.0218	98.0218	98.0218	98.0218

Table 5
Total component reliability for the PV systems for a period of 20 years of operations [in %]. Note that 0% does not mean that the overall PV system is failed, it means that at least one component of the PV system is failed.

Power (kW)	100	200	500	1000	1500	2000	2500
PV modules	66.2218	43.8532	12.9654	1.6512	0.2141	0.0273	0.0035
String protection	63.9737	40.9264	10.9255	1.1707	0.1279	0.0137	0.0015
DC switch	96.3455	92.8245	83.0149	71.5288	59.3796	49.2939	40.9213
Inverter	8.2085	0.6738	0.0004	0.0000	0.0000	0.0000	0.0000
AC circuit breaker	70.1574	49.2205	16.9968	4.1177	0.6999	0.1190	0.0202
Grid protection	70.1574	70.1574	70.1574	70.1574	70.1574	70.1574	70.1574
AC switch	99.7893	99.7893	99.7893	99.7893	99.7893	99.7893	99.7893
Differential circuit breaker	70.1574	70.1574	70.1574	70.1574	70.1574	70.1574	70.1574
Connector (couple)	98.7069	97.4305	93.7525	87.8455	82.3574	77.1684	72.3473
Battery system	99.9923	99.9846	99.9616	99.9232	99.8848	99.8464	99.8080
Charge controller	67.0587	67.0587	67.0587	67.0587	67.0587	67.0587	67.0587

$$R_{tot} = \exp\left(\sum_{i=1}^{n} m_i \lambda_i t_i\right) \tag{28}$$

where m_i is the total number of components (i.e. 8702 PV modules for 2 MW PV system), λ_i is the failure rate of component i, n is the total number of different components, and t is the study time of the reliability analysis. For instance, the total reliability of the PV modules for a 2 MW system (8702 PV modules) for one year (365 days × 8.5 h = 3102.5 h) is:

$$R_{PV,tot} = \exp\left(-1 \times 8702 \times 0.0152 \times 10^{-6} \times 3102.5\right) = 0.663405 \tag{29}$$

The total component reliability for the PV system over one year and over 20 years of operation was calculated using Equation (28), (see Tables 4 and 5). Additionally, the failure rate for the battery system that consists of series and parallel paths was determined using Equation (17); for instance, the total reliability of the battery system for a 100 kW PV system is represented as:

$$R_{Battery-system} = 1 - \left(1 - R^2\right)^8 = 1.328 \times 10^{-9} \tag{30}$$

4. Simulation and results

By substituting the failure rates listed in Table 3 into Equation (28), the total component reliability of PV systems for one year and 20 years of operation was estimated (See Tables 4 and 5). The component reliabilities decreased as the PV power output increased; for instance, after one year for a 200 kW system, the PV modules had a 95.9622% probability of operating without failures, while the inverter had only a 77.8801% probability. For a 2.5 MW system, the PV modules had a 59.8988% probability of operating without failures, while the inverter had only a 4.9787% probability (see Table 4). However, for 20 years of operation, the reliability declined quickly. For a 200 kW system, the PV modules were 43.8532% reliable, while the inverter was only 0.6738% reliable. For a 2.5 MW system, the PV modules had only a 0.0035% probability of operating correctly, while the inverter was not reliable, with a 0% probability of operating without failures (see Table 5).

A reliability of 0% means that there is at least one component with a failure, which induces the failure of the overall PV system.

The overall system reliability for one year and for 20 years of operation is reported in Table 6.

To obtain useful information from this study, the Fussel–Vesely method was used. This method accounts for the effect of each single component on the overall system reliability, which can be calculated as:

$$FV = \left[1 - \left(\exp\left(-\sum_{i=1}^{n} m_i \lambda_i t_i\right)\right)\right] \tag{31}$$

For instance, the Fussel–Vesely of the string protection for a 100 kW system (23 string protections) for 20 years of operation (365 days × 20 years × 8.5 h = 62,050 h) is:

$$FV = \left[1 - \left(\exp\left(-1 \times 23 \times 0.313 \times 10^{-6} \times 62050\right)\right)\right] = 0.36023 \tag{32}$$

The Fussel–Vesely method reveals the impact of the PV modules, string protections, DC switches, inverters, AC circuit breakers,

Table 6
The overall system reliability for a period of one and 20 years of operations [in %]. Note that 0% does not mean that the overall PV system is failed, it means that at least one component of the PV system is failed.

Power (kW)	100	200	500	1000	1500	2000	2500
Reliability (in%, 1 year)	78.3716	64.9282	36.9896	16.6818	6.5229	2.5457	0.9954
Reliability (in%, 20 years)	0.7641	0.0177	0.0000	0.0000	0.0000	0.0000	0.0000

Table 7
Results of Fussel–Vesely for one year of operations.

Power (kW)	100	200	500	1000	1500	2000	2500
PV modules	2.0397	4.0378	9.7101	18.5503	26.4591	33.6595	40.1012
String protection	2.2087	4.3687	10.4796	19.9387	28.3288	35.9019	42.6191
DC switch	0.1860	0.3716	0.9264	1.6614	2.5724	3.4750	4.3693
Inverter	11.7503	22.1199	46.4738	67.5347	82.6225	90.6985	95.0213
AC circuit breaker	1.7565	3.4822	8.4795	14.7424	21.9719	28.5883	34.6436
Grid protection	1.7565	1.7565	1.7565	1.7565	1.7565	1.7565	1.7565
AC switch	0.0105	0.0105	0.0105	0.0105	0.0105	0.0105	0.0105
Differential circuit breaker	1.7565	1.7565	1.7565	1.7565	1.7565	1.7565	1.7565
Connector (couple)	0.0651	0.1301	0.3220	0.6459	0.9658	1.2875	1.6054
Battery system	0.0004	0.0008	0.0019	0.0038	0.0058	0.0077	0.0096
Charge controller	1.9782	1.9782	1.9782	1.9782	1.9782	1.9782	1.9782

Table 8
Results of Fussel–Vesely for 20 years of operations.

Power (kW)	100	200	500	1000	1500	2000	2500
PV modules	33.7782	56.1468	87.0346	98.3488	99.7859	99.9727	99.9965
String protection	36.0263	59.0736	89.0745	98.8293	99.8721	99.9863	99.9985
DC switch	3.6545	7.1755	16.9851	28.4712	40.6204	50.7061	59.0787
Inverter	91.7915	99.3262	99.9996	100	100	100	100
AC circuit breaker	29.8426	50.7795	83.0032	95.8823	99.3001	99.8810	99.9798
Grid protection	29.8426	29.8426	29.8426	29.8426	29.8426	29.8426	29.8426
AC switch	0.2107	0.2107	0.2107	0.2107	0.2107	0.2107	0.2107
Differential circuit breaker	29.8426	29.8426	29.8426	29.8426	29.8426	29.8426	29.8426
Connector (couple)	1.2931	2.5695	6.2475	12.1545	17.6426	22.8316	27.6527
Battery system	0.0077	0.0154	0.0384	0.0768	0.1152	0.1536	0.1920
Charge controller	32.9413	32.9413	32.9413	32.9413	32.9413	32.9413	32.9413

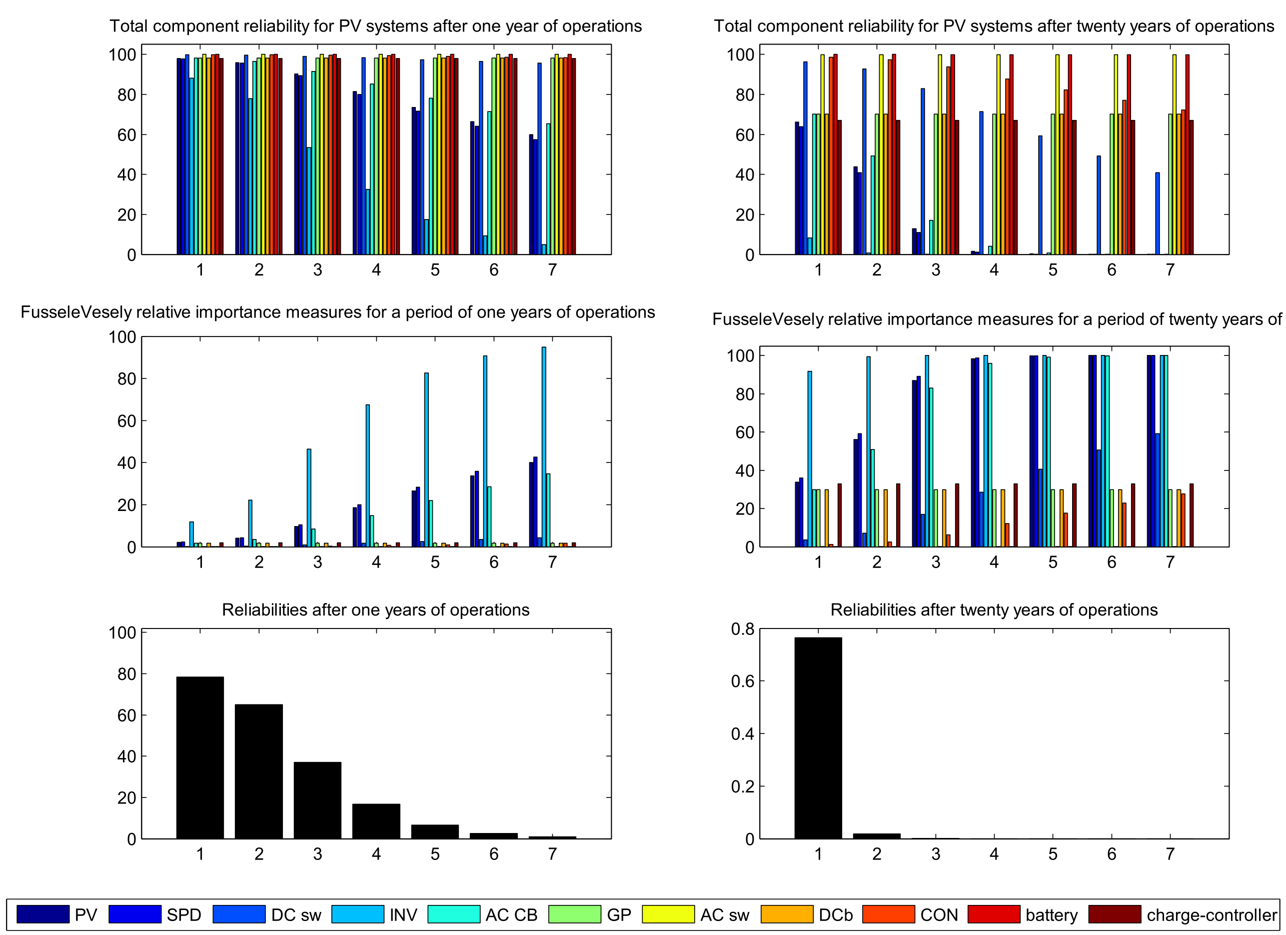

Fig. 5. The all results of reliability for seven PV systems.

Table 9
Critical component priorities.

Priority	Component
1	Inverter
2	String protection
3	PV modules
4	AC circuit breaker
5	DC switch
6	Charge controller
7	Grid protection
7	Differential circuit breaker
9	Connector (couple)
10	AC switch
11	Battery system

grid protection, AC switches, differential circuit breaker, connectors, battery systems and charge controllers on the overall system reliability of large-scale PV systems.

The Fussel–Vesely results for one year and for 20 years of operation appear in Tables 7 and 8.

Fig. 5 displays all of the results of this study for seven PV system tests, numbered 1 to 7.

5. Conclusion

Photovoltaic systems are fairly reliable and usually can be trusted to operate without any failures. However, like any other system, they may fail, so the effects of failures should be calculated. This paper described a method for evaluating the reliability of the components in large-scale PV systems. The ranking of the most critical components appears in Table 9. The component that fails the most must be able to be replaced or repaired quickly after a failure. PV systems could have a high rate of availability under frequent maintenance, but frequent maintenance is not an optimal solution. Maintenance strategies can be optimized to reduce the associated costs. It is necessary to point out that although the scope of this paper was based on unrepairable components, the proposed method can be further considered with the repair time in order to evaluate the system economic losses. In addition, Future work will focus on which types of maintenance are appropriate for the components of large-scale PV systems.

Acknowledgment

The authors gratefully acknowledge the associate editor, and anonymous referees for their valuable comments and expertise in versioning this study.

References

[1] A. Golnas, IEEE J. Photovoltaics 3 (1) (2013) 416–421.
[2] J. Sawin, E. Martinot, Renewables 2010 Global Status Report, Renewable Energy Policy Network, 2010 (Report No.1).
[3] Zhao Zheng-ming, Liu Jian-zheng, Solar Power Generation and Application [M], Science Press, Beijing, 2005.
[4] World's Largest Photovoltaic Power Plants, PVresources, 2009 (online). Available at: http://www.pvresources.com/en/top50pv.php.
[5] W.C. Sinke, Int. Sustain. Energy Rev. 1 (2009).
[6] L.H. Stember, Sol. Cells 3 (3) (1981) 26985.
[7] M.A. Hamdy, M.E. Beshir, S.E. Elmasry, Appl. Energy 33 (4) (1989) 25363.
[8] N.A. Al-Rawi, M.M. Al-Kaisi, D. Asfer, Sol. Energy Mater. Sol. Cells 31 (4) (1994) 45568.
[9] N.A. Al-Rawi, M.M. Al-Kaisi, D. Asfer, Sol. Energy Mater. Sol. Cells 31 (4) (1994) 46980.
[10] W. Zhou, H. Yang, Z. Fang, Appl. Energy 84 (2007) 11871198.
[11] A. Jain, S.C. Tripathy, R. Balasubramanian, Energy Convers. Manag. 36 (3) (1995) 1839.
[12] T. Kerekes, E. Koutroulis, D. Sera, R. Teodorescu, M. Katsanevakis, IEEE J. Photovoltaics 3 (2) (2013) 814–822.
[13] L.H. Stember, W.R. Huss, M.S. Bridgman, IEEE Trans. Reliab. R-31 (3) (1982) 296303.
[14] P.R. Mishra, J.C. Joshi, Energy Convers. Manag. 37 (9) (1996) 137182.
[15] A. Urbina, T.L. Paez, C. O'Gorman, P. Barney, R.G. Jungst, D. Ingersoll, J. Power Sources 80 (1999) 30–38.
[16] S. Islam, A. Woyte, R. Belmans, P.J.M. Heskes, P.M. Roiji, Renew. Energy 31 (2006) 115781.
[17] N.K. Gautam, N.D. Kaushika, Sol. Energy 72 (2) (2002) 12941.
[18] T. Oozeki, T. Yamada, K. Kato, T. Yamamoto, in: Proc. ISES Solar World Congress, 2007, 16281632.
[19] W.M. Rohouma, I.M. Molokhiab, A.H. Esuri, Desalinisation 209 (2007) 1228.
[20] M.A. Eltawil, Z. Zhao, Renew. Sustain. Energy Rev. 14 (2010) 11229.
[21] Z. Gabriele, M. Christophe, M. Jens, Renew. Energy 36 (2011) 2334–2340.
[22] W. Muneer, K. Bhattacharya, C.A. Caizares, IEEE Trans. Power Syst. 26 (4) (2011) 25472555.
[23] J.V. Paatero, P.D. Lund, Renew. Energy 32 (2) (Feb. 2007) 216234.
[24] C.H. Lin, W.L. Hsieh, C.S. Chen, C.T. Hsu, T.T. Ku, C.T. Tsai, IEEE Trans. Ind. Appl. 47 (4) (2011) 1884–1891.
[25] J. Phillips, Renew. Sustain. Energy Rev. 27 (2013) 435444.
[26] P. Zhang, W. Li, S. Li, Y. Wang, W. Xiao, Appl. Energy 104 (2013) 822833.
[27] I. Das, K. Bhattacharya, C. Caizares, W. Muneer, IEEE Trans. Sustain. Energy 4 (2) (2013) 370–378.
[28] G. Levitin, L. Xing, S.V. Amari, Y. Dai, Reliab. Eng. Syst. Saf. 119 (2013) 218228.
[29] L. Xing, G. Levitin, Reliab. Eng. Syst. Saf. 112 (2013) 145153.
[30] G. Levitin, L. Xing, H. Ben-Haim, D. Yuanshun, IEEE Trans. Reliab. 62 (3) (2013) 637–647.
[31] S. Reed, J.D. Andrews, S.J. Dunnett, IEEE Trans. Reliab. 60 (1) (2011) 70–79.
[32] M.T. Lazim, M. Zeidan, Electr. Power Energy Syst. 47 (2013) 7884.
[33] H.S. Rauschenbach, Solar Cell Array Design Handbook, Van Nostrand Reinhold, New York, 1980.
[34] B.S. Borowy, Z.M. Salameh, IEEE Trans. Energy Convers. 11 (2) (1996) 367–375.
[35] Reliability Prediction of Electronic Equipment, MIL-HDBK-217F, 217F Notice 1, 217F Notice 2, Department of Defense, Washington DC USA, 19919295.
[36] L.K. Nkhonjera, Simulation and Performance Evaluation of Battery Based Stand-alone Photovoltaic Systems of Malawi (M.Sc. thesis), Environmental Sustainable Development, National Central University, 2009.
[37] F.M. Akhmedjanov, Reliability Databases: State-of-the-art and Perspectives, Ris National Laboratory, Pitney Bowes Management Services Denmark A/S. Roskilde, 2001, ISBN 87-550-2809-8.
[38] C.O. Smith, Introduction to Reliability in Design, McGraw Hill, New York, 1976.
[39] T. Gonen, Electric Power Distribution System Engineering, California State University Sacramento, California, 2008.
[40] H. Pham, Handbook of Reliability Engineering, Springer, 2003.
[41] M. Cepin, Assessment of Power System Reliability-Methods and Applications, Springer, London Dordrecht Heidelberg New York, 2011.
[42] Richard E. Brown, Electric Power Distribution Reliability, second ed., Taylor and Francis Group, Boca Raton, London, New York, 2009.
[43] D.F. Haasl, N.H. Roberts, W.E. Vesely, F.F. Goldberg, Fault Tree Handbook, Washington D.C, USA, 1981.
[44] R.M. Sinnamon, J.D. Andrews, Reliab. Eng. Syst. Saf. 58 (1997) 89–96.